Journal of Zhejiang University-SCIENCE A (Applied Physics & Engineering)
ISSN 1673-565X (Print); ISSN 1862-1775 (Online)
www.jzus.zju.edu.cn; www.springerlink.com
E-mail: jzus@zju.edu.cn

Temperature-induced structural static responses of a long-span steel box girder suspension bridge*

Lin-ren ZHOU[1], Lan CHEN[†‡1], Yong XIA[2], Ki Young KOO[3]

[1]*School of Civil Engineering and Transportation, South China University of Technology, Guangzhou 510641, China*

[2]*Department of Civil and Environmental Engineering, The Hong Kong Polytechnic University, Kowloon, Hong Kong, China*

[3]*College of Engineering, Mathematics and Physical Sciences, University of Exeter, Exeter, UK*

[†]E-mail: chenlan@scut.edu.cn

Received Sept. 22, 2019; Revision accepted Feb. 2, 2020; Crosschecked June 15, 2020

Abstract: Temperature is a significant load on bridges, particularly for long-span steel box girder bridges. This study investigates the temperature-induced static responses of a long-span suspension bridge under real service environmental conditions using numerical simulations and field measurements. Detailed 2D finite element (FE) models of a typical section for the box girder, main cable, hanger, tower column, and crossbeam are constructed. The thermal boundary conditions are determined strictly according to the surrounding environments of a typical sunny day and applied to the FE models. A transient heat-transfer analysis is performed and the time-dependent temperature and its distribution on the bridge are obtained. In addition, a fine, 3D FE model of the bridge is developed for a structural analysis. The calculated temperatures are applied to the 3D model and the temperature-induced structural responses are simulated. The simulated temperatures and the associated static responses have good agreement with the measured counterparts and support the numerical simulation method. The main cable and bridge deck make the greatest contributions to the temperature effects on the suspension bridge. The static responses of bridge caused by the design vehicle load are also calculated. The daily variation of the temperature-induced static responses is comparable with, even higher than, that of the design vehicle load.

Key words: Long-span suspension bridge; Temperature effect; Static response; Vehicle load; Field monitoring
https://doi.org/10.1631/jzus.A1900490 **CLC number:** TU311.4; U448.25

1 Introduction

Bridges are designed for a long service life but are inevitably degraded by harsh environments, particularly bridges with long spans in maritime settings. These harsh environments reduce a bridge's performance and may result in catastrophic collapse. Of the loads bridges are designed to handle, temperature is widely recognized as having a significant and negative effect. The variation of temperature and of its distribution caused by the changes in the meteorological environment of a bridge, subsequently affect its structural static and dynamic properties and can lead to responses such as movement, deformation, stress, cracking, reaction forces, and changes in connection and boundary conditions. The daily cycle of temperature variation may also lead to fatigue damage. In fact, many numerical and field studies on bridges indicate that the temperature-induced structural responses are more significant than those imposed by operational loads (Priestley, 1976, 1978; Kennedy and Soliman, 1987; Salawu, 1997). Temperature consumes a significant proportion of the

‡ Corresponding author
* Project supported by the National Key Research and Development Program of China (No. 2017YFC0803300) and the Science and Technology Planning Project of Guangdong Province (No. 2014A020218003), China
ORCID: Lin-ren ZHOU, https://orcid.org/0000-0002-9053-7922

bridge's carrying capacity and so degrades the structure's performance. Temperature effects are key issues in the life cycle of a bridge and they must be appropriately considered during design, construction, and operational maintenance.

Temperature effect on bridges has attracted considerable attention and has been a leading topic for inquiry since the 1960s (Zuk, 1965). The analysis of the temperature effect on bridges has focused on two main topics: structural temperature and temperature-induced responses. Obtaining time-dependent structural temperature and distribution is the basis for the subsequent temperature effect analysis. Field monitoring is the most common method of data collection and is prominent in the literature (Priestley, 1976, 1978; Kennedy and Soliman, 1987). Direct measurements may be used for analysis and to derive mathematical expressions, and they have created a vast literature investigating bridge temperature effects using data-driven approaches based on field measurements (Roberts-Wollman et al., 2002; Kromanis and Kripakaran, 2017; Zhou et al., 2018; Zhou and Sun, 2019).

Structural health monitoring (SHM) technologies have been widely used for important infrastructures (Ou and Li, 2010; Huang et al., 2015; Wang et al., 2018; Zhang et al., 2019). For large and long-span bridges, monitoring in the field is possible since SHM systems are commonly installed. However, the measuring points in these systems are limited and they cannot fully, or precisely, capture the temperature distribution of the entire bridge. Monetary and time costs make in-situ monitoring infeasible for every typical bridge. However, numerical simulation is an efficient and low-cost approach to calculate structural temperature and temperature-induced responses. The first investigations of structural temperature assumed a 1D and linear distribution (Emerson, 1973; Hunt and Cooke, 1975; Kehlbeck, 1975). However, 1D linear models cannot adequately represent the temperature distribution of large and complex bridges such as the long-span steel box girder bridges. The development of 2D models was the result (Elbadry and Ghali, 1983; Tong et al., 2001). Nevertheless, achieving a desirable level of accuracy for large bridges with complex configurations and long spans is still challenging. With the rapid development of computational techniques and an increasing demand for structural analysis, advanced numerical simulation methods using commercial finite element (FE) software have been widely adopted, a development that provides a comprehensive and highly accurate analysis for the temperature behavior of bridges, especially large and long-span bridges (Xia et al., 2013; Tayşi and Abid, 2015; Zhou et al., 2016; Zhu and Meng, 2017). Until now, these studies have focused only on structural temperatures. The effects of these temperature loads on structural responses have not been investigated using numerical methods.

Temperature imparts a major environmental action on bridges (Zhou and Yi, 2013). Variations in temperature and in its distribution will change the properties of the bridge's geometry and its materials, as well as the boundary conditions, generating static and dynamic structural responses. Temperature-induced responses are highly dependent on the bridge types and structural materials. Typically, significant temperature effects are observed in large and long-span bridges, such as long-span cable-stayed and suspension bridges, and the effects are even greater in box girder and steel constructions (Xu et al., 2010; Xia et al., 2013; Westgate et al., 2015; Tomé et al., 2018; Yang et al., 2018). Temperature-induced stress and displacement (or movement) of bridges have been widely investigated since the 1970s (Emerson, 1979; Dilger et al., 1983; Mirambell and Aguado, 1990; Moorty and Roeder, 1992). Fujino et al. (2000) pointed out that temperature was the major factor affecting configurations of long-span suspension bridges. Deng et al. (2010) monitored a long-span suspension bridge in the field and found the annual change in the displacement at the end of the bridge girder was more than 50 cm. Kromanis et al. (2016) found significant temperature-induced displacements and forces imposed at the bearings of a seven-span steel box girder bridge which were significantly greater than these due to vehicle load.

The accurate assessment of temperature effects is essential to ensure reliability and safety. Many of the assessment and design methods for bridge temperature effects have been proposed and investigated based on temperature-induced static responses. Roeder (2003) proposed a design method for expansion joints to accommodate temperature-induced movements of different bridge types, and compared

the method with existing specifications and field observations from the American Association of State Highway and Transportation Officials. Ni et al. (2007) evaluated the conditions of bridge expansion joints using long-term field measurements of movement and temperature. Duan et al. (2011) investigated the correlation between strain and temperature in a tied-arch bridge, and quantified the temperature effects based on the measured strain response. Wang et al. (2015) conducted an assessment of a steel-truss arch girder bridge and observed that changes in static strain were mainly caused by variations in temperature, and the temperature-induced strain showed an apparent linear correlation with the temperature. Xia et al. (2017) presented a new damage identification method using the measured temperature-induced strain in a long-span suspension bridge. However, research on the effects of temperature on long-span bridges has mainly focused on global structural responses and has not yet revealed temperature behaviors at the component level, nor how the components interact.

Similar to vehicle, wind, and seismic loading, structural temperature imposes a loading action on bridges. However, any temperature effect is imposed slowly due to the intrinsically gradual change of the ambient temperature. Within a short period of time, temperature-induced structural responses are not as dramatic as those caused by vehicle, wind, or seismic loads, and yet temperature effects exist at every component of a bridge at every moment. The temperature effect may lead to damage, age construction materials, reduce a bridge's carrying capacity, and degrade its performance. However, a bridge seldom collapses solely because of temperature effects, and it is this understanding that drives the discussions in this study. This study focuses on how severe temperature-induced impacts might be on a bridge. We partially address the issue by investigating the temperature-induced static responses of a long-span steel box girder suspension bridge using numerical simulation and field monitoring. The list here identifies the structure of this paper:

1. The long-span suspension bridge considered in this study and its SHM system are introduced.

2. Fine FE models for thermal and structural analyses are constructed and described.

3. The structural temperatures of the entire bridge on a sunny day are calculated and compared to the measurements to validate the numerical model and methodology.

4. The temperature-induced static responses of the suspension bridge are calculated and the results are compared to measurements and simulations under the design vehicle load.

The conclusion offers suggestions for measuring and mitigating temperature-induced static responses of long-span box girder suspension bridges.

2 Engineering background

2.1 Humber Bridge

The Humber Bridge is located at the estuary of the River Humber, England. Construction began in March 1973 and the bridge opened to traffic on June 24, 1981. The Humber Bridge has a total length of 2220 m with an asymmetric layout of 280 m (north), 1410 m, and 530 m (south), as shown in Fig. 1. The 1410 m main span made the bridge the longest suspension bridge in the world for 17 years. The bridge is currently the 10th longest of its type.

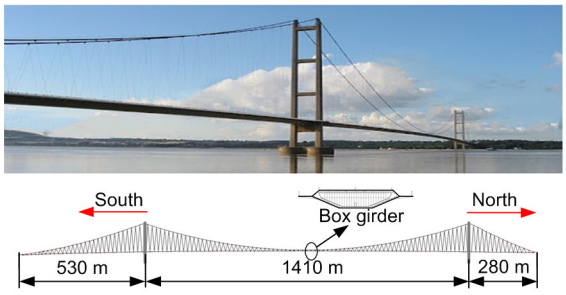

Fig. 1 Photograph and diagram of the Humber Bridge

The bridge carries a dual, two-lane highway, footpaths, and cycle tracks. The steel box girder was designed to be a streamlined box, 4.8-m high and with an 18-m wide upper surface covered with 41-mm thick rubberized bitumen asphalt. Two flanges, each 3-m wide, cantilever outwards from the boxes. They carry footpaths and cycle tracks. The north tower is located at the shore and the south tower is located in the river, 500 m from the shoreline. The towers are 155.5 m above the piers, and each tower has two hollow-section columns connected by four cross-beams, as shown in Fig. 1. The top and bottom

crossbeams are hollow-sections. The main cables were designed for a maximum pull of 19400 t and each cable consists of 14948 parallel, galvanized drawn wires of 5-mm diameter. The bridge's asymmetry means the suspension cable of the northern span is relatively steeper and has a greater tension. There are 800 additional wires in the cable fixing the main anchorage and the tower saddles on this northern aspect (Fisher, 1982).

2.2 Humber Bridge SHM system

The bridge's SHM system has three subsystems: sensor system, network system, and data management system. The sensor system has four components based on the characteristics being detected: (1) meteorological parameters measured include air temperature, wind speed, and wind direction; (2) accelerometers at the mid-span detect dynamic responses to vibrations; (3) static responses are gauged by four extensometers in each tower column, an inclinometer at the mid-span measures lateral inclination of the bridge deck, and two global position system (GPS) receivers are fixed on the suspension cables at the mid-span; (4) structural temperature is detected by six thermocouples. The six thermocouples monitor the temperature of the box girder section at the mid-span. Two temperature sensors are installed at the middle of the left lane of the northbound carriageway to obtain data on the surface temperature of the asphalt and the ground temperature at the interface between steel and paved asphalt. The final four temperature sensors were placed on the top, bottom, east, and west of the interior surface of the box girder at the mid-span.

3 FE models

3.1 FE model for thermal analysis

For slender structures and structural components, the cross-sectional temperatures along the longitudinal plane are assumed to be constant. This permits 2D section FE models to be used to calculate the temperatures of the box girder, main cable, hanger, tower column, and crossbeam. In this study, the FE models for thermal analysis are established using the ANSYS software package. Fig. 2 shows the FE models of typical sections of the suspension bridge. All the FE models are developed using PLANE55 elements with different material properties according to the as-built situation. PLANE55 is a 2D element with four nodes and each node has a single degree of freedom (DOF) of temperature. It is equipped with thermal conduction capability and is suitable for both steady-state and transient thermal analyses.

The box girder, including the air of the inside hollow, is entirely modeled to achieve a complete thermal equilibrium system, as shown in Fig. 2. The thermal radiation interaction (thermal radiation boundary condition) of the interior surface is calculated by AUX12 Radiation Matrix method using super-element MATRIX50. The thermal analysis FEs of the main cable and the hanger are similar but with different sizes and material properties. The covering layer is modeled in accordance with the real situation. The spaces between the parallel steel stranded wires are filled with air, and it is difficult to model them separately. Therefore, the steel stranded wires of the cable are simulated as homogeneous material with

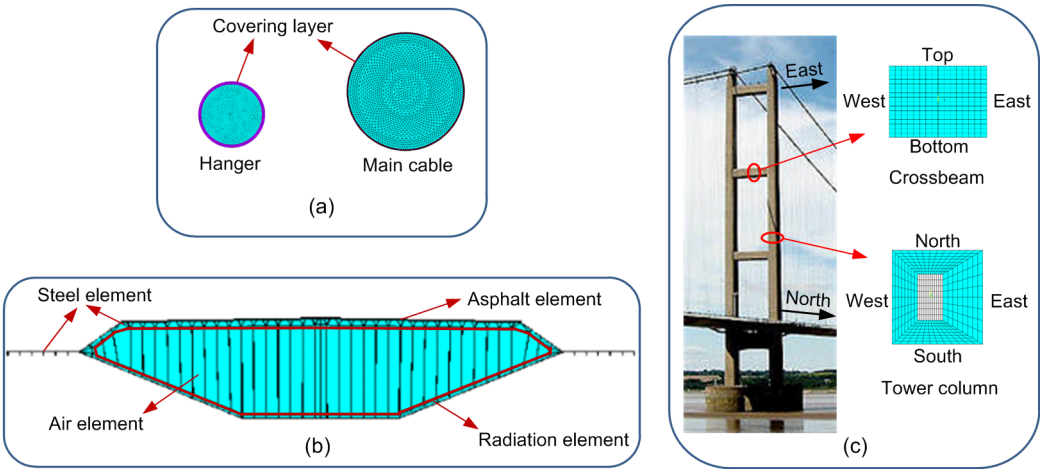

Fig. 2 The 2D FE models for the thermal analysis: (a) cables; (b) deck; (c) tower

equivalent material parameters of thermal properties (Chen et al., 2017). The detailed FE models of concrete tower column and crossbeam are also constructed for temperature analysis, as shown in Fig. 2.

3.2 FE model for structural analysis

The FE model of the suspension bridge for structural analysis is developed using the 3D modeling capability of ANSYS. Fig. 3 shows the structural FE model and its details, which consists of 117578 elements. The steel box girder is modeled using SHELL181 elements. The pavement layer on the upper deck is considered to contribute weight and we ignore its contribution to stiffness. The concrete towers are constructed using SOLID65 elements. The suspension cables and hangers are modeled using LINK181 elements. The tower and main cable are connected at a same node on the top of tower. At the end of the bridge girder, spring bearings using COMBIN14 elements are modeled to simulate the boundary conditions.

4 Thermal analysis of the suspension bridge

The energy exchanges between the bridge system and the surrounding environment consist of heat convection, heat conduction, and thermal radiation. These processes are complex and are significantly affected by the outside environmental factors. In order to calculate the structural temperatures using FE method, the thermal boundary conditions for thermal analysis should be firstly determined. The authors had previously carried out a comprehensive investigation on the numerical simulation of temperature for the box girder of this suspension bridge (Zhou et al., 2016). In this study, the temperatures of the other components, such as main cable, hanger, and tower, are calculated. Subsequently, by applying these temperatures in the structural FE model, the temperature-induced structural responses of the entire bridge can be analyzed.

A typical sunny day, July 24, 2012, was selected for this study. The field weather conditions are shown in Fig. 4. The wind speed, wind direction, and air temperature were collected by the weather station at the mid-span of the bridge. Cloud cover was obtained from the meteorological measurements at the Humberside Airport, about 18 km by road from the bridge. The maximum cloud cover during daylight hours was 25%, which is considered a clear day. Types of radiation and thermal boundary conditions are calculated using corresponding theoretical and empirical formulas. For brevity, the computation processes are not described here, but can be found in related research (Kehlbeck, 1975; Zhou et al., 2016). The main material parameters for thermal analysis are summarized in Table 1 (Kehlbeck, 1975; Tong et al., 2001; Xia et al., 2013).

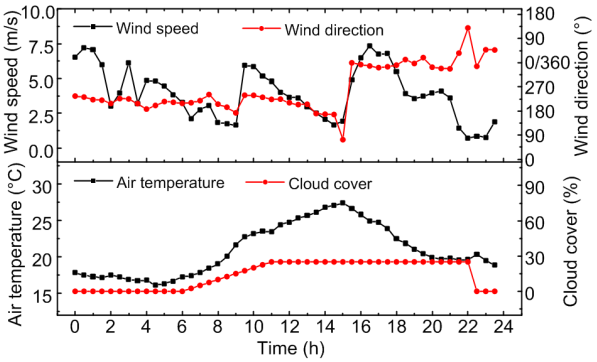

Fig. 4 Field weather conditions for July 24, 2012

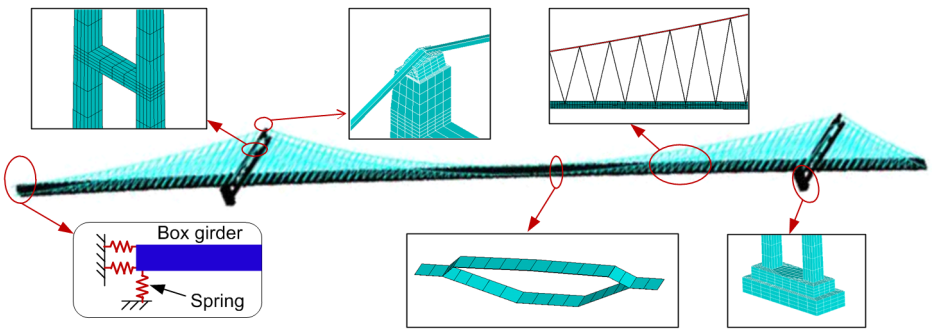

Fig. 3 FE model for structural analysis

The calculated surface temperatures of the east tower column and crossbeam are presented in Fig. 5. The temperature variation of the observed surfaces shows a high correlation with the air temperature. It can be observed that the structural temperature decreased slightly before reaching a minimum in the early morning, then increased to a peak in the early afternoon, and finally fell again in the evening. The temperature variations exactly represent the effect of solar radiation on the structural surfaces. The eastern surface of the tower column received more solar radiation than other surfaces in the morning, had a relatively high temperature and reached its maximum earlier. In the afternoon, the western and southern surfaces absorbed most of the solar radiation and the temperature reached 28 °C. The time when the maximum temperature is recorded for each tower column indicates the sun's motion from east to west. The sun's transit explains the higher temperature recorded on the top surface of the crossbeam compared to the other surfaces. In contrast, the bottom surface had the lowest temperature because it was shaded from the sun. The thermal analysis results of the tower column and crossbeam indicate good consistency with the changing environments.

Table 1 Material parameters for thermal analysis

Parameter	Value			
	Concrete	Steel	Asphalt	Air
Density (kg/m^3)	2400	7850	1530	0.0012
Heat capacity (J/(kg·°C))	925	460	1075	1.007
Thermal conductivity (W/(m·°C))	2.710	60	1.800	0.026
Emissivity coefficient	0.88	0.80	0.92	0
Absorptivity coefficient	2.930	0.398	0.434	0.036

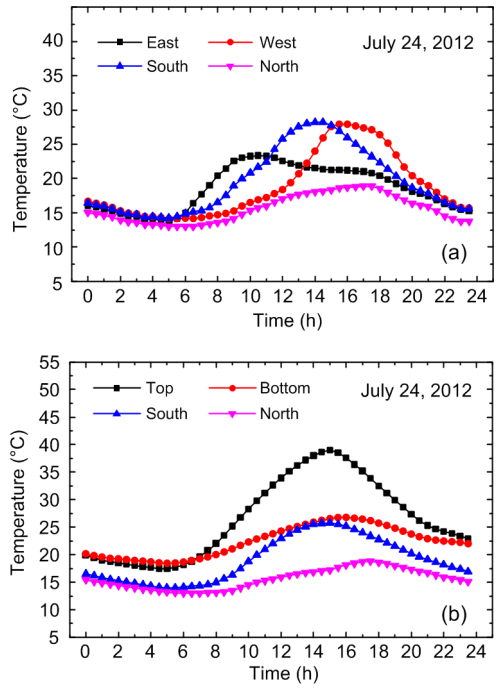

Fig. 5 Calculated surface temperatures of the east tower column (a) and crossbeam (b)

Thermal boundary conditions of the main cable and the hanger were calculated and applied to the corresponding FE models. Transient thermal analysis was performed to obtain the temperatures. The temperature distribution of the main cable at 15:00 is shown in Fig. 6. The top-most, western surface received more solar radiation, resulting in a higher temperature. At the peak temperature, energy is transferred from outside to inside. The temperatures in the hanger show results similar to the main cable. The main cable and hanger are slender structures with low bending stiffness; the cross-sectional temperature gradient has a limited effect on their mechanical properties. Therefore, the average temperature is used for temperature-induced structural response analysis. The average temperatures of the main cable and hanger are shown in Fig. 7. The hanger had higher temperatures and greater variation than the main cable due to its smaller mass and thinner covering layer, which makes it more sensitive to ambient temperature and solar radiation.

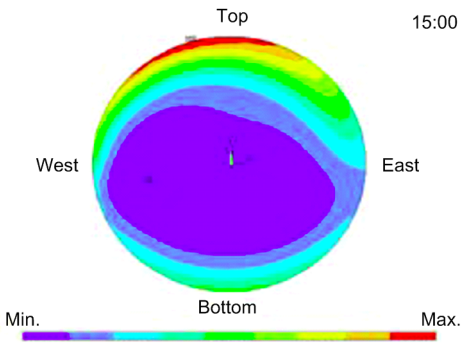

Fig. 6 Temperature field of the main cable at 15:00

5 Structural static response analysis

5.1 Static responses due to design vehicle load

To assess the daily temperature-induced static response of the Humber suspension bridge, we analyzed the static responses to design vehicle load. The discussed static responses are shown in Fig. 8, including the vertical displacement (D in short) and inclination (I in short) of the bridge deck at the mid-span, strains on the mid-span box girder section (SB1–SB3), strains on the main cable at different points (SC1–SC4), strains on the hanger at different points (SH1–SH4), and strains on the tower column near the bottom crossbeam (ST1 and ST2). According to BS 5400-2:2006 (BSI, 2006), the standard for construction of steel, concrete, and composite bridges, a uniformly distributed load of 17.3 kN/m is applied to each lane of the bridge deck. At the mid-span, a concentrated load of 120 kN is applied. The static responses are calculated by structural analysis using the structural FE model. The vehicle load-induced static responses are listed in Tables 2 and 3. The vertical displacement at the mid-span was up to 4 m. The top and bottom plates of the box girder mainly supported the vehicle loads. The lateral deck inclination was negligible since the vehicle load was symmetrical. The main cable had considerable strain, and the main cable section nearer to the tower had larger strain. Observing the hanger, the hanger at the mid-span had the largest strain.

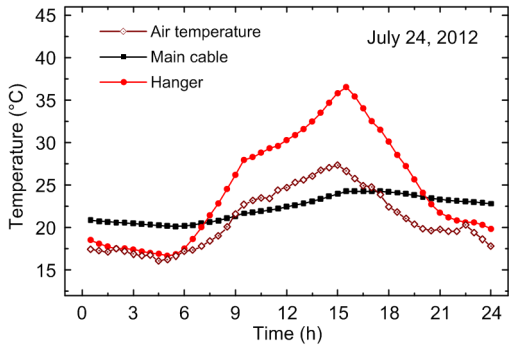

Fig. 7 Average temperatures of main cable and hanger

5.2 Temperature-induced static responses

The temperatures of the suspension bridge during a typical sunny day (July 24, 2012) were obtained by numerical simulation using the fine 2D FE models described in Section 3. The simulated temperatures were applied to the structural FE model to analyze the temperature-induced static responses. The node temperatures of the box girder and tower were transferred to the structural FE model as temperature loads.

Table 2 Static responses of the box girder section at the mid-span due to the design vehicle load

Displacement (D in short) (m)	Inclination (I in short) (‰)	Strain (με)		
		SB1	SB2	SB3
4.03	0.01	17.9	28.9	0.4

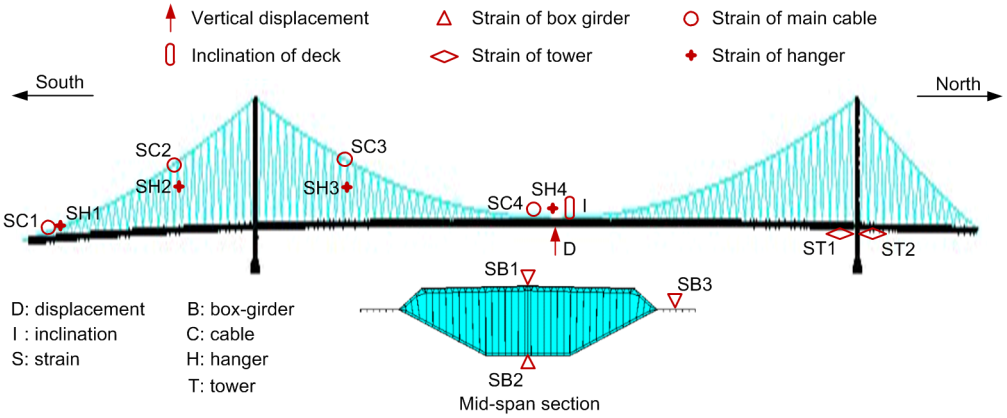

Fig. 8 Notations and locations of the discussed static responses

Table 3 Strains on bridge components due to the design vehicle load (unit: με)

Main cable				Hanger				Tower	
SC1	SC2	SC3	SC4	SH1	SH2	SH3	SH4	ST1	ST2
211.0	649.6	719.3	506.1	68.6	207.9	256.4	260.8	25.9	92.7

The average temperatures are utilized as temperature loads for the main cable and hanger. Structural analysis was performed to obtain temperature-induced static responses. Below, we present a discussion of the temperature-induced vertical displacement and lateral inclination at the mid-span, and the temperature-induced strain on the box girder, main cable, hanger, and tower.

5.2.1 Temperature-induced vertical displacement at the mid-span

From midnight onwards, the variation in temperature-induced vertical displacement at the mid-span is shown in Fig. 9. The calculated results have very good agreement with the field measurements. Vertical displacement increased slightly and reached a maximum at about 5:00, dropped to a minimum at about 16:00, and then increased across the remainder of the period. The total daily change is about 50 cm, which represents 12.4% of the displacement caused by the design vehicle load. The vertical displacement displays a reverse tendency to the structural temperature. That is because the bridge component sizes expand and the material elastic modulus decreases as temperature increases. Fig. 10 shows the contributions of different components to temperature-induced vertical displacement. It can be seen that the main cable and box girder are the greatest contributors, accounting for more than 90% of the displacement. Changing bridge girder temperature makes a significant contribution to the vertical displacement at the mid-span. Bridge deck elevation at the mid-span is higher than that at either end (the difference is about 18 m), and as temperatures increase, the lengths of the girders expand, causing the girder elevation near the mid-span to fall.

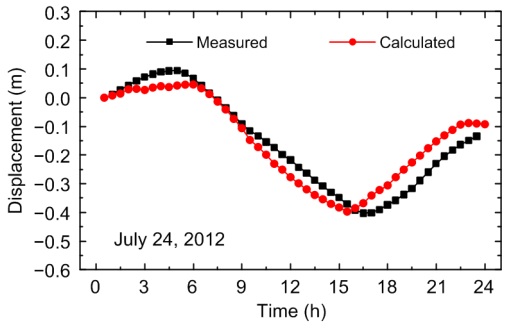

Fig. 9 Temperature-induced vertical displacement at the mid-span

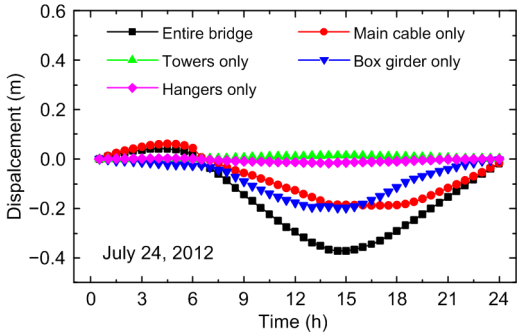

Fig. 10 Contributions of the bridge's components to temperature-induced vertical displacement

5.2.2 Temperature-induced lateral inclination of the bridge deck at the mid-span

The lateral deck (east-west) inclination of two days (July 24 and May 30, 2012) under different wind loads is calculated and discussed. The numerical and measured results are shown in Fig. 11. They show a similar tendency, which indicates a high correlation with the simulated transverse temperature difference (TTD) of the box girder; inclination synchronously varies with the change in TTD. The inclination appeared as a positive value (higher on the east side of deck than the west side) after the sunrise in the morning because the east side of the box girder received more solar radiation. Similarly, from afternoon to sunset, the west side of the box girder had higher

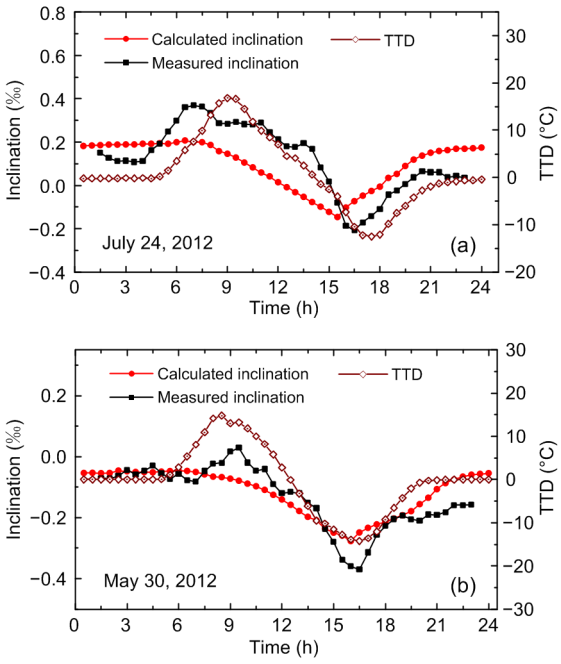

Fig. 11 Inclination and TTD of the box girder at the mid-span on July 24 (a) and May 30 (b) in 2012

temperature than the east side, which generated a negative value of the deck inclination. However, there are certain differences between the numerical and measured data because the deck inclination is also significantly affected by the wind. The average wind speeds on July 24 and May 30 in 2012 were 3.9 m/s and 2.5 m/s, respectively. The model better predicts temperature-induced inclination on the day when with lower wind speed.

For long-span suspension bridge, deck inclination is influenced by temperature differences, wind, and vehicle load. Vehicle load is known to create transient episodes of deck inclination. Significant ongoing daily variation in deck inclination is largely generated by temperature and wind. The total changes of measured inclination were 0.58‰ and 0.40‰ with respect to July 24 and May 30, respectively. The corresponding temperature-induced inclinations were 0.35‰ and 0.23‰, which were 60.34% and 57.5% of the measurements, respectively. The TTD of the box girder is a major cause of lateral inclination.

5.2.3 Temperature-induced strain on the box girder

The temperature-induced strains and the average temperatures of the box girder section at the mid-span are shown in Fig. 12. The simulated results correspond exactly to the changes in the environments. Structural temperature and strain decreased slightly and reached the minimum in the early morning, increased dramatically to peak in the early afternoon, and then fell throughout the evening. The variation of the top (SB1, SB3) and bottom (SB2) strains of the box girder showed the opposite tendency since the temperature and temperature gradient caused bending of the box girder. The increase of temperature led to expansion of the top plate and shrinkage of the bottom plate. The variation amplitudes of SB1 and SB2 on this day were about equal to 150 με, yet significantly greater than the strains attributed to the design vehicle load, 17.9 με and 28.9 με, for points SB1 and SB2, respectively. The box girder flange (SB3) recorded the biggest temperature-induced strain with a total change of 200 με. However, the strain due to the design vehicle load was only 0.4 με. The results demonstrate that the temperature-induced strain on the box girder is much greater than that from vehicle load. For some secondary or accessory components, temperature may become the dominant load action during their service life.

5.2.4 Temperature-induced strain in the main cable

The temperature behavior of the main cable strongly affects the structural responses of the bridge, including characteristics such as cable sag, tower deviation, and box girder deflection. The temperature-induced strains at the four positions (notated as SC1–SC4 in Fig. 8) and average temperatures of the main cable are shown in Fig. 13. The temperature-induced strain decreased as temperature increased. The total daily changes of the temperature-induced strains at the four points were 47.6 με (SC1), 435.7 με (SC2), 471.9 με (SC3), and 331.9 με (SC4). They are sorted in descending order as SC3, SC2, SC4, and SC1, which is in accordance with the slope of the main cable at these four locations, possibly because the main cable segment with a deeper slope is more sensitive to the vertical hanger actions. Compared with the strains due to the design vehicle load as listed in Table 3, the changing amplitudes of temperature-induced strains were 22.60% (SC1), 67.07% (SC2), 65.61% (SC3), and 65.58% (SC4) of the strains caused by the design vehicle load.

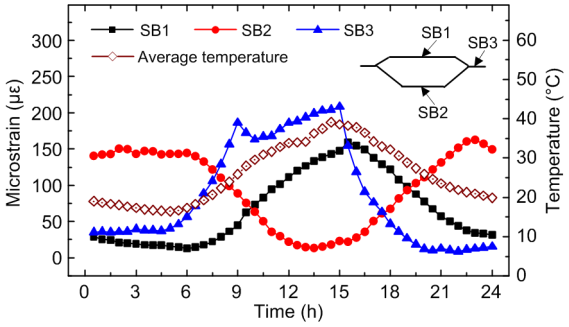

Fig. 12 Variation in temperature-induced strains and the average temperature of the box girder

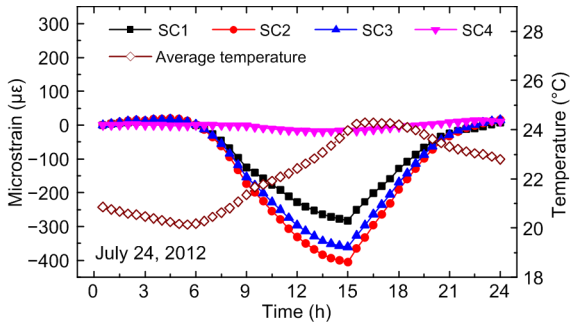

Fig. 13 Variation in temperature-induced strains and the average temperature of the main cable

5.2.5 Temperature-induced strain on the hanger

The temperature-induced behavior of a single hanger is linked to its length and boundary conditions. A longer hanger and a stiffer boundary condition will typically lead to bigger temperature-induced responses. Four hangers (SH1–SH4 in Fig. 8) of the bridge are selected to investigate the temperature-induced strain. Taking the start time as reference point, the variations of the temperature-induced strain on July 24, 2012 are presented in Fig. 14. All the temperature-induced strains of the four hangers synchronously changed with the change of temperature. However, the amplitudes of variation were different. Hanger SH4 at the mid-span had the largest variation of 225.5 με. However, hanger SH1 near the end of bridge, with similar length to hanger SH4, had a daily variation of only 73.3 με. Such a difference was because the hanger SH4, with a relatively larger dip angle at the mid-span, had to resist a greater relative displacement difference between the suspension cable and the bridge deck. Compared with the hanger strains caused by the design vehicle load, the daily changes of the temperature-induced strains were 86.46% (SH4), 42.98% (SH3), 28.28% (SH2), and 106.84% (SH1) of the strains due to the design vehicle load. Temperature has a greater effect on the short hanger than on the long hanger.

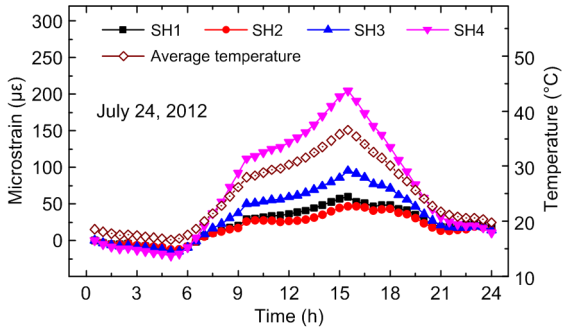

Fig. 14 Variation in temperature-induced strains and the average temperature of the hangers

5.2.6 Temperature-induced strain on the tower

The towers of a suspension bridge support the main cables, bear entire loads, and deliver them to the foundations. The hollow concrete towers of a suspension bridge are typically hundreds of meters high. The temperature effects on towers should be sufficiently considered for the construction and in-service stages of a suspension bridge. However, the structural system and behavior of the bridge tower during construction (without main cable) and in operation are different. Hence, the temperature-induced strains of the two cases are simulated and discussed in this section. Taking the start time as reference point, the strains extracted from the column surface points near the bottom crossbeam are shown in Fig. 15. The point ST1 is on the south side and ST2 is on the north side. Focusing on the case of the construction stage, the temperature-induced strains (ST1-C and ST2-C) had the same variation tendency with the change of structural temperature, but the south side (ST1-C) had larger changing amplitude than the north side (ST2-C) since the south side surface received more solar radiation. Observing the strains at the operation stage (ST1-S and ST2-S), it is interesting to note that they had reverse variation tendencies during the daytime. The reason is that the temperature behavior of a tower is caused not only by the temperatures of the tower itself, but also the temperature effects of other components such as the main cables. The strain of the north-side point ST2-S decreased with the rise in temperature of the whole bridge, because the slackening of the main cable made the tower bend to the north. Subsequently, the north-side tower column is relatively compressed. Compared with the tower strains caused by the design vehicle load, the variation amplitudes of the temperature-induced strain were 105.01% (ST1) and 46.93% (ST2) of those caused by the design vehicle load, with an average of 75.97%. It can be seen that the temperature effects on the tower are considerable.

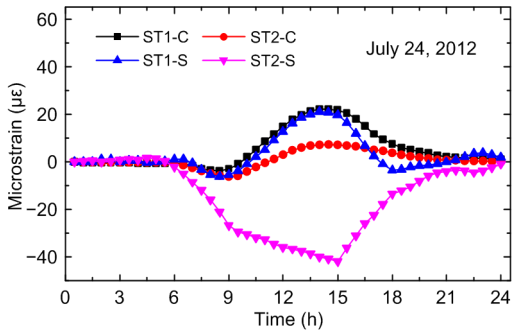

Fig. 15 Temperature-induced strains of the tower at the stages of construction and operation

6 Conclusions

Temperature effects are key issues for bridges, especially large and long-span bridges. Temperature distribution and variation influence the bridge's structural behavior, as has been widely recognized and verified by field monitoring. However, accurately analyzing the temperature-induced structural behavior of long-span bridges is a challenge because of their complex configurations, uncertainties during service, and the changing of meteorological environments. This study carries out a comprehensive investigation of temperature-induced static responses based on a long-span steel box girder suspension bridge. High-resolution FE models of this bridge for thermal analysis and structural analysis are constructed separately. Thermal boundary conditions are determined taking account of the real service environments, and then the transient thermal analysis is performed to obtain the time-dependent temperatures. The static responses caused by temperatures and design vehicle load are calculated and compared. The numerical results are also verified through a comparison with the field measurements. Based on the simulated and measured temperature effects of the long-span steel box girder suspension bridge, we draw the following conclusions:

1. The daily change in temperature-induced vertical displacement at the mid-span is considerable, about one-tenth of the displacement caused by the design vehicle load. Bridge deck inclination is mainly generated by TTD and the wind, but temperature accounts for the major portion of the daily changes.

2. The temperature-induced strain varies greatly on the box girder on a day-to-day basis. Temperature strain can be several times larger than the strain caused by the design vehicle load. The flanges of the box girder withstand the greatest temperature-induced strains, whereas the strain from design vehicle load is considered to be negligible. The results indicate that temperature effects could be the major load action for a bridge's secondary structures.

3. The strains caused by temperature at different main cable locations very much depend on the cable slope. Steeper cables are associated with larger temperature-induced strains. The temperature-induced strains at the selected four points are on average 66% of the strains caused by the design vehicle load.

4. The temperature-induced strain of a hanger highly depends on its length and boundary conditions. Longer hangers with more rigid boundary constraints will create greater temperature-induced strains. However, the short hanger at the mid-span has the greatest temperature-induced strain, due to the large relative displacement difference between its ends.

5. Temperature-induced strain in the tower column is caused not only by exposure to ambient heat but also the temperature effects impacting on the main cables. The variation in temperature-induced strain within the tower column near the bottom crossbeam is comparable to the strain caused by the design vehicle load.

The temperature effects on the static responses of a long-span steel suspension bridge are significant. For some components, the temperature-induced static responses were greater than those caused by the design vehicle load. It is worth noting that the structural temperatures used in this study are from a single day. Since the weather varies greatly within weeks, months, and even over years, temperature effects are likely to be more extreme than the effects measured in this study. Temperature effects consume a considerable amount of a bridge's bearing capacity, vary considerably over time, and have long-term consequences. The temperature effects on long-span suspension bridges should be given sufficient consideration during bridge design, and, once in service, continual monitoring and assessment.

Contributors

Lan CHEN designed the research. Lin-ren ZHOU processed the corresponding data and wrote the first draft of the manuscript. Yong XIA helped to organize the manuscript. Ki Young KOO provided the field measurements. Lin-ren ZHOU revised and edited the final version.

Conflict of interest

Lin-ren ZHOU, Lan CHEN, Yong XIA, and Ki Young KOO declare that they have no conflict of interest.

References

BSI (British Standards Institution), 2006. Steel, Concrete and Composite Bridges–Part 2: Specification for Loads, BS 5400-2:2006. BSI, London, UK.

Chen L, Liang CF, Huang ZG, et al., 2017. Numerical simulation on the temperature behavior of the main cable for suspension bridge. *Health Monitoring of Structural and Biological Systems*, 10170:1017038.

https://doi.org/10.1117/12.2259941

Deng Y, Ding YL, Li AQ, 2010. Structural condition assessment of long-span suspension bridges using long-term monitoring data. *Earthquake Engineering and Engineering Vibration*, 9(1):123-131. https://doi.org/10.1007/s11803-010-9024-5

Dilger WH, Ghali A, Chan M, et al., 1983. Temperature stresses in composite box girder bridges. *Journal of Structural Engineering*, 109(6):1460-1478. https://doi.org/10.1061/(asce)0733-9445(1983)109:6(1460)

Duan YF, Li Y, Xiang YQ, 2011. Strain-temperature correlation analysis of a tied arch bridge using monitoring data. Proceedings of the International Conference on Multimedia Technology, p.6025-6028. https://doi.org/10.1109/ICMT.2011.6002979

Elbadry MM, Ghali A, 1983. Temperature variations in concrete bridges. *Journal of Structural Engineering*, 109(10): 2355-2374. https://doi.org/10.1061/(asce)0733-9445(1983)109:10(2355)

Emerson M, 1973. The Calculation of the Distribution of Temperature in Bridges. Technical Report No. LR 561, Transport and Road Research Laboratory, Berkshire, UK.

Emerson M, 1979. Bridge Temperatures for Setting Bearings and Expansion Joints. Technical Report No. SR 479, Transport and Road Research Laboratory, Wokingham, UK.

Fisher D, 1982. Design and construction of the Humber Bridge. *Physics Education*, 17(5):198-202. https://doi.org/10.1088/0031-9120/17/5/302

Fujino Y, Murata M, Okano S, et al., 2000. Monitoring system of the Akashi Kaikyo Bridge and displacement measurement using GPS. Proceedings of SPIE's 5th Annual International Symposium on Nondestructive Evaluation and Health Monitoring of Aging Infrastructure, p.229-236. https://doi.org/10.1117/12.387814

Huang XH, Dyke S, Xu ZD, 2015. An in-time damage identification approach based on the Kalman filter and energy equilibrium theory. *Journal of Zhejiang University-SCIENCE A (Applied Physics & Engineering)*, 16(2): 105-116. https://doi.org/10.1631/jzus.A1400163

Hunt B, Cooke N, 1975. Thermal calculations for bridge design. *Journal of the Structural Division*, 101(4):1763-1781.

Kehlbeck F, 1975. Einfluss der Sonnenstrahlung bei Brückenbauwerken. Werner-Verlag, Düsseldorf, Germany (in German).

Kennedy JB, Soliman MH, 1987. Temperature distribution in composite bridges. *Journal of Structural Engineering*, 113(3):65-78. https://doi.org/10.1061/(asce)0733-9445(1987)113:3(475)

Kromanis R, Kripakaran P, 2017. Data-driven approaches for measurement interpretation: analysing integrated thermal and vehicular response in bridge structural health monitoring. *Advanced Engineering Informatics*, 34:46-59. https://doi.org/10.1016/j.aei.2017.09.002

Kromanis R, Kripakaran P, Harvey B, 2016. Long-term structural health monitoring of the Cleddau Bridge: evaluation of quasi-static temperature effects on bearing movements. *Structure and Infrastructure Engineering*, 12(10):1342-1355. https://doi.org/10.1080/15732479.2015.1117113

Mirambell E, Aguado A, 1990. Temperature and stress distributions in concrete box girder bridges. *Journal of Structural Engineering*, 116(9):2388-2409. https://doi.org/10.1061/(asce)0733-9445(1990)116:9(2388)

Moorty S, Roeder CW, 1992. Temperature-dependent bridge movements. *Journal of Structural Engineering*, 118(4): 1090-1105. https://doi.org/10.1061/(asce)0733-9445(1992)118:4(1090)

Ni YQ, Hua XG, Wong KY, et al., 2007. Assessment of bridge expansion joints using long-term displacement and temperature measurement. *Journal of Performance of Constructed Facilities*, 21(2):143-151. https://doi.org/10.1061/(asce)0887-3828(2007)21:2(143)

Ou JP, Li H, 2010. Structural health monitoring in mainland China: review and future trends. *Structural Health Monitoring*, 9(3):219-231. https://doi.org/10.1177/1475921710365269

Priestley MJN, 1976. Design thermal gradients for concrete bridges. *New Zealand Engineering*, 31(9):213-219.

Priestley MJN, 1978. Design of concrete bridges for temperature gradients. *Journal of American Concrete Institute*, 75(5):209-217.

Roberts-Wollman CL, Breen JE, Cawrse J, 2002. Measurements of thermal gradients and their effects on segmental concrete bridge. *Journal of Bridge Engineering*, 7(3): 166-174. https://doi.org/10.1061/(asce)1084-0702(2002)7:3(166)

Roeder CW, 2003. Proposed design method for thermal bridge movements. *Journal of Bridge Engineering*, 8(1):12-19. https://doi.org/10.1061/(ASCE)1084-0702(2003)8:1(12)

Salawu OS, 1997. Detection of structural damage through changes in frequency: a review. *Engineering Structures*, 19(9):718-723. https://doi.org/10.1016/S0141-0296(96)00149-6

Tayşi N, Abid S, 2015. Temperature distributions and variations in concrete box-girder bridges: experimental and finite element parametric studies. *Advances in Structural Engineering*, 18(4):469-486. https://doi.org/10.1260/1369-4332.18.4.469

Tomé ES, Pimentel M, Figueiras J, 2018. Structural response of a concrete cable-stayed bridge under thermal loads. *Engineering Structures*, 176:652-672. https://doi.org/10.1016/j.engstruct.2018.09.029

Tong M, Tham LG, Au FTK, et al., 2001. Numerical modelling for temperature distribution in steel bridges. *Computers & Structures*, 79(6):583-593. https://doi.org/10.1016/S0045-7949(00)00161-9

Wang GX, Ding YL, Sun P, et al., 2015. Assessing static performance of the Dashengguan Yangtze Bridge by

monitoring the correlation between temperature field and its static strains. *Mathematical Problems in Engineering*, 2015:946907. https://doi.org/10.1155/2015/946907

Wang QW, Zhong DH, Wu BP, et al., 2018. Construction simulation approach of roller-compacted concrete dam based on real-time monitoring. *Journal of Zhejiang University-SCIENCE A (Applied Physics & Engineering)*, 19(5):367-383. https://doi.org/10.1631/jzus.A1700042

Westgate R, Koo KY, Brownjohn J, 2015. Effect of solar radiation on suspension bridge performance. *Journal of Bridge Engineering*, 20(5):04014077. https://doi.org/10.1061/(ASCE)BE.1943-5592.0000668

Xia Q, Cheng YY, Zhang J, et al., 2017. In-service condition assessment of a long-span suspension bridge using temperature-induced strain data. *Journal of Bridge Engineering*, 22(3):04016124. https://doi.org/10.1061/(ASCE)BE.1943-5592.0001003

Xia Y, Chen B, Zhou XQ, et al., 2013. Field monitoring and numerical analysis of Tsing Ma Suspension Bridge temperature behavior. *Structural Control and Health Monitoring*, 20(4):560-575. https://doi.org/10.1002/stc.515

Xu YL, Chen B, Ng CL, et al., 2010. Monitoring temperature effect on a long suspension bridge. *Structural Control and Health Monitoring*, 17(6):632-653. https://doi.org/10.1002/stc.340

Yang DH, Yi TH, Li HN, et al., 2018. Monitoring and analysis of thermal effect on tower displacement in cable-stayed bridge. *Measurement*, 115:249-257. https://doi.org/10.1016/j.measurement.2017.10.036

Zhang XS, Chen JQ, Wei JH, 2019. Condition-based scheduled maintenance optimization of structures based on reliability requirements under continuous degradation and random shocks. *Journal of Zhejiang University-SCIENCE A (Applied Physics & Engineering)*, 20(4):272-289. https://doi.org/10.1631/jzus.A1800578

Zhou GD, Yi TH, 2013. Thermal load in large-scale bridges: a state-of-the-art review. *International Journal of Distributed Sensor Networks*, 9(12):217983. https://doi.org/10.1155/2013/217983

Zhou GD, Yi TH, Chen B, et al., 2018. Modeling deformation induced by thermal loading using long-term bridge monitoring data. *Journal of Performance of Constructed Facilities*, 32(3):04018011. https://doi.org/10.1061/(ASCE)CF.1943-5509.0001154

Zhou LR, Xia Y, Brownjohn JMW, et al., 2016. Temperature analysis of a long-span suspension bridge based on field monitoring and numerical simulation. *Journal of Bridge Engineering*, 21(1):04015027. https://doi.org/10.1061/(ASCE)BE.1943-5592.0000786

Zhou Y, Sun LM, 2019. A comprehensive study of the thermal response of a long-span cable-stayed bridge: from monitoring phenomena to underlying mechanisms. *Mechanical Systems and Signal Processing*, 124:330-348. https://doi.org/10.1016/j.ymssp.2019.01.026

Zhu JS, Meng QL, 2017. Effective and fine analysis for temperature effect of bridges in natural environments. *Journal of Bridge Engineering*, 22(6):04017017. https://doi.org/10.1061/(ASCE)BE.1943-5592.0001039

Zuk W, 1965. Thermal behavior of composite bridges-insulated and uninsulated. *Highway Research Record*, (76):231-253.

中文概要

题　目： 大跨度钢箱梁悬索桥温度所致结构静力响应

目　的： 温度对大跨度桥梁的力学性能影响显著。针对大跨度钢箱梁悬索桥，本文采用数值方法分析日温度变化引起的结构静力响应，对比设计车荷载，以评估温度静力效应的影响。

创新点： 1. 基于数值方法对比大跨度悬索桥温度静力效应与设计车荷载效应，评估温度效应的影响；2. 阐明悬索桥主要构件温度效应对总体温度效应的贡献及相互之间的影响。

方　法： 1. 建立现场环境和结构响应的结构健康监测系统，并进行长期监测；2. 通过精细化有限元分析方法实现桥梁温度荷载和温度效应的精准数值计算。

结　论： 1. 温度对大跨度悬索桥跨中位移的影响明显，其一天的变化约是设计车荷载位移的 10%；箱型主梁横向温差是导致桥面横向倾斜的主要因素。2. 箱梁温度应力显著大于车荷载引起的应力；部分次要构件的温度应力成为主要荷载效应。3. 主缆竖向倾角越大，温度应力越大；吊杆温度效应主要受其长度和两端相对变形的影响。4. 桥塔温度效应不仅受其自身温度的影响，也会受到来自主缆温度响应的较大影响。5. 本文结论是基于一天温度变化的影响，而温度效应在更大时间尺度上的影响会更为严重。

关键词： 大跨度悬索桥；温度效应；静态响应；车荷载；现场监测